 © 2012 Uspekhi Fizicheskikh Nauk, Russian Academy of Sciences

CONFERENCES AND SYMPOSIA

PACS numbers: 01.10.Fv, **01.60. + q**, **01.65. + g**, 04.80.Nn, **07.60. – j**, **42.60. – v**, 91.25.Mf, **94.30. – d**, **96.60. – j**

Commemoration of the centenary of the birth of Academician V V Migulin

(Scientific session of the Physical Sciences Division of the Russian Academy of Sciences, 28 September 2011)

DOI: 10.3367/UFNe.0182.201203e.0323

The scientific session of the Physical Sciences Division of the Russian Academy of Sciences (RAS) commemorating the 100th anniversary of the birthday of Academician V V Migulin was held on September 28, 2011 at the conference hall of the P N Lebedev Physical Institute of the RAS.

The following reports were put on the session agenda posted on the website www.gpad.ac.ru of the RAS Physical Sciences Division:

(1) **Gulyaev Yu V** (V A Kotel'nikov Institute of Radioengineering and Electronics, RAS, Moscow) "Radiophysical methods in biomedical research";

(2) **Vyatchanin S P** (M V Lomonosov Moscow State University, Moscow) "Parametric oscillatory instability in laser gravitational antennas";

(3) **Kuznetsov V D** (N V Pushkov Institute of Terrestrial Magnetism, Ionosphere and Radiowave Propagation, RAS, Troitsk, Moscow region) "Solar-terrestrial physics and its applications".

The opening address and articles written on the base of the oral reports 2 and 3 are published below.

PACS numbers: **01.60. + q**, **01.65. + g**
DOI: 10.3367/UFNe.0182.201203f.0323

Opening address

Yu V Gulyaev

Today's session is devoted to the memory of Vladimir Vasil'evich Migulin. Organizers asked me to say a few words about him because he worked for some time with us at the Institute of Radioengineering and Electronics (IRE).

V V Migulin was born in 1911 in the town of Sereda (renamed Furmanov) in the Ivanovskaya region. In 1932, he graduated from the Leningrad Polytechnic Institute, and started his career in 1934 in N D Papaleksi's group at the Leningrad Electrophysical Institute. After the Academy of Sciences and most of its research institutes moved to Moscow in 1934, V V Migulin began to work at the P N Lebedev Physical Institute of the RAS under the supervision of L I Mandelshtam and N D Papaleksi, where he developed various parametric amplifiers, generators, and converters — it was he, in fact, who really launched this whole field.

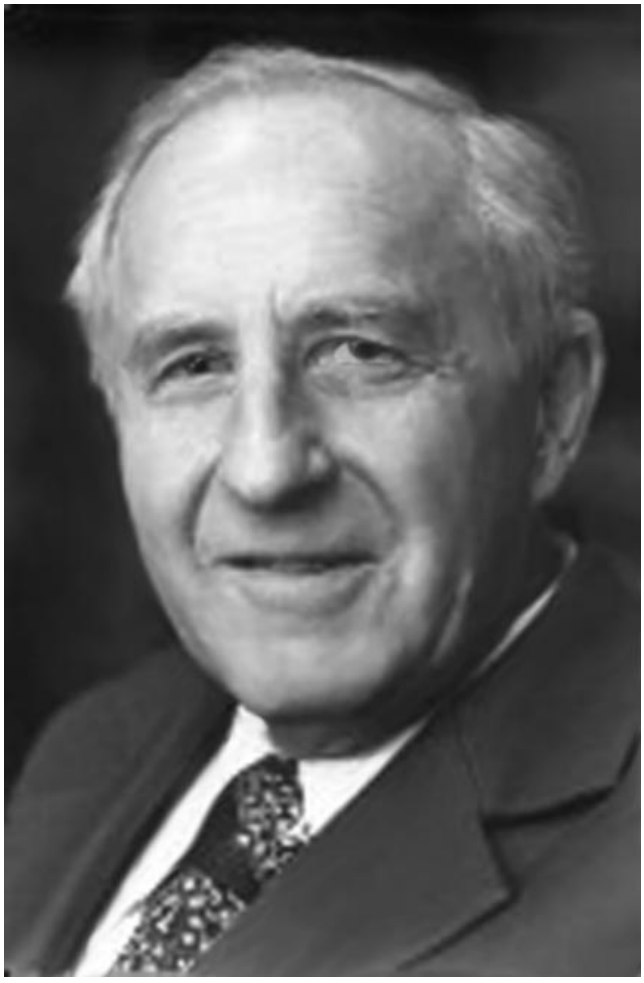

Vladimir Vasil'evich Migulin
(10.07.1911 – 22.09.2002)

At the next stage, V V Migulin redirected his research to studying the propagation of radio waves. He began working

Yu V Gulyaev V A Kotel'nikov Institute of Radioengineering and Electronics, RAS, Moscow, Russian Federation
E-mail: gulyaev@cplire.ru

Uspekhi Fizicheskikh Nauk **182** (3) 323 – 336 (2012)
DOI: 10.3367/UFNr.0182.201203e.0323
Translated by V I Kisin and E N Ragozin; edited by A Radzig

Uspekhi Fizicheskikh Nauk **182** (3) 323 – 324 (2012)
DOI: 10.3367/UFNr.0182.201203f.0323
Translated by V I Kisin; edited by A Radzig

on radiointerferometry, which made it possible to determine the phase structure and velocity of propagation of waves along the Earth's surface.

During WWII, he developed radio navigation and radar systems for the air force.

In 1951, V V Migulin was appointed Director of the Sukhumi Physical-Technical Institute, where work on the Soviet Atomic project was conducted, including work on rocket design. The research staff of the Institute involved many German scientists brought to the USSR from defeated Germany.

I will make a short detour here. It is likely that many of you knew the German scientist Klaus Thiessen, or heard about him. In 1953–1954, he was a student at Moscow State University. At the time, I was a student at the Moscow Institute of Physics and Technology (FizTekh), and we were acquainted. Well, his father Peter Adolf Thiessen was the person who developed the fuel for the German V-2 rocket. As you know, once WWII ended, the Americans got hold of rocket designer von Braun, and we Soviets got hold of P A Thiessen, Hitler's former science advisor, and this very P A Thiessen, essentially the technical director of the Sukhumi Institute, then worked for Stalin.

Between 1957 and 1959, V V Migulin was the acting deputy to the IAEA Director General in Vienna.

In 1962–1969, V V Migulin headed the Department of Parametric and Electronic Devices at the RAS Institute of Radioengineering (IRE). He appears to be the first person to bring attention in 1968 to applying a physical novelty, SQUIDs, as potential quantum interference sensors of magnetic fields. Our first SQUIDs were designed under his guidance at this Department. He was able to assemble a team of experts known to many of you: V P Koshelets, G A Ovsyannikov, and some others. That is all his scientific school, and today it is to a great extent thanks to V V Migulin and the school he created that the IRE RAS has stayed at the forefront of SQUID development and applications. My subsequent talk on biomagnetic measurements will partly be devoted to applications of SQUIDs possessing extremely high sensitivity.

In 1969, V V Migulin became Director of the RAS Institute of Terrestrial Magnetism, Ionosphere and Radiowave Propagation (IZMIRAN); he headed this Institute for 20 years. V V Migulin made a great contribution to progress in a new field of research — solar-terrestrial physics. He was also a scientific leader of the Interkosmos-19 program; the pioneering results of space exploration which made us all so proud were actually obtained under his guidance.

The spectrum of V V Migulin's interests in science was exceptionally wide. I even remember, although I cannot expand on this topic here, that he once described how in some obscure way he and Zel'dovich together had even discovered somewhere quarks. In addition, Vladimir Vasil'evich never stopped doing work of great social significance. He was Deputy Secretary-Academician of the Physical Sciences Division of the RAS for nearly 30 years. It is fair to say that in reality he shared the management of the Division with the Secretary-Academician.

V V Migulin also took part in the work of international organizations. One such organization was URSI (the French abbreviation of Union Radio-Scientifique Internationale). Even though a large number of international organizations exist in the fields of radiophysics, radio electronics, etc., most of them are applications-oriented. For example, in the long run the IEEE (Institute of Electrical and Electronics Engineers) is precisely the institute for engineers in the fields of radio electronics, electrical engineering, etc., and thus mostly concerns itself with the practical applicability of the results of research. URSI is actually the only organization focusing primarily on fundamental problems. Well, for five years Migulin was the Vice-President of the entire URSI, and for 20 years he headed the URSI Russian Committee. At the moment, I am in fact his legal successor, as I now head the same URSI committee. Consequently, I am well informed about his activities in the international arena as well.

Vladimir Vasil'evich Migulin had an exceptionally wonderful personality. Very important among his characteristic features was the absolute reliability of his word; he was a model workaholic and was always very upset if he was late arriving for anything — his time was planned to the minute, and not only regarding his job but in dealing with people as well. When Vladimir Vasil'evich talked to you, he listened attentively, looking straight at you, and always tried hard to do something and help. Even after resigning from the IRE directorship in 1988, when I became IRE Director, he would be a regular visitor, enquiring about progress in the Department of Superconductor Electronics, which was very much his brainchild; he was always very close to it.

The memory of him is very dear to us, very clear and very warm, and I think most people who knew him feel that way. He was a wonderful person.

PACS numbers: 04.80.Nn, **07.60.–j**, **42.60.–v**
DOI: 10.3367/UFNe.0182.201203g.0324

Parametric oscillatory instability in laser gravitational antennas

S P Vyatchanin

1. Introduction

I had the honor of knowing Vladimir Vasil'evich Migulin when I was an undergraduate student, a postgraduate student, and then a staff member in the chair headed by him. Unfortunately, I did not maintain close contact with him, but I was well aware of the high prestige he enjoyed among the chair staff members.

V V Migulin is known for his work on parametric processes [1–3]. The subject of my report is the undesirable parametric instability effect, which is also inherently parametric.

An obvious illustration of parametric oscillatory instability is the model of a two-circuit parametric amplifier (Fig. 1) which consists of two parallel oscillatory circuits connected with a variable coupling capacitor $C_0(t) = C_0 + \delta C \cos \omega_0 t$ [4]. As is well known, the operation of the parametric amplifier becomes unstable for sufficiently strong pumping (i.e., when the modulation part δC of the coupling capaci-

S P Vyatchanin M V Lomonosov Moscow State University, Moscow, Russian Federation
E-mail: svyatchanin@phys.msu.ru

Uspekhi Fizicheskikh Nauk **182** (3) 324 – 327 (2012)
DOI: 10.3367/UFNr.0182.201203g.0324
Translated by E N Ragozin; edited by A Radzig

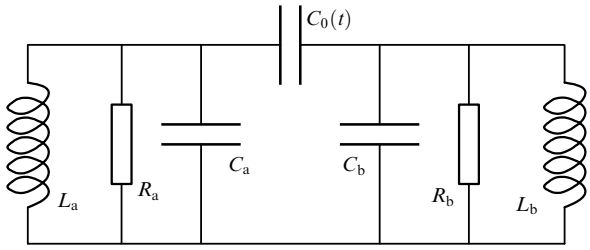

Figure 1. Two-circuit parametric amplifier model. The partial circuit frequencies ω_a, ω_b and the modulation frequency ω_0 of the coupling capacitance $C_0(t) = C_0 + \delta C \cos \omega_0 t$ obey the relationship $\omega_0 \simeq \omega_a + \omega_b$.

tance is large enough). The instability condition for a perfect synchronism (i.e., when $\omega_0 = \omega_a + \omega_b$) has the following form:

$$\frac{\delta C^2}{C_a C_b} > \frac{\gamma_a \gamma_b}{\omega_a \omega_b}\,, \qquad \gamma_a \equiv \frac{R_a}{2L_a}\,, \qquad \gamma_b \equiv \frac{R_b}{2L_b}\,. \tag{1}$$

It is also known that parametric pumping is responsible for the insertion of *antidamping*, and that condition (1) describes a situation where the inserted damping is higher than the intrinsic one [5].

2. Parametric oscillatory instability

To qualitatively consider the phenomenon of parametric oscillatory instability (POI), we address ourselves to the configuration of a Fabry–Perot resonator (Fig. 2) which is excited through resonance pumping at the frequency ω_0. One of the resonator mirrors is mobile and comprises a mechanical oscillator of frequency ω_m. Let there exist a Stokes optical-resonator mode with an eigenfrequency ω_1, so that the following condition is satisfied:

$$\omega_0 \simeq \omega_1 + \omega_m\,. \tag{2}$$

In this case, a parametric interaction between these modes is possible, which may give rise to parametric instability [6–10]. In the presence of small oscillations in the optical Stokes mode, a ponderomotive force emerges which acts on the mobile mirror at the difference frequency $\omega_0 - \omega_1 \simeq \omega_m$, which *resonantly* drives mechanical oscillations. On the other hand, small mechanical oscillations of the mirror owing to the Doppler effect give rise to the mirror-reflected waves with combination frequencies $\omega_0 \pm \omega_m$. One of these waves (with the frequency $\omega_0 - \omega_m \simeq \omega_1$) resonantly excites oscillations in the optical Stokes mode. With increasing pump power at the frequency ω_0, the stated mechanisms evidently result in progressively greater energy transfer. In accordance with the Manley–Rowe relations, the energy of the pump wave will be transferred to the optical Stokes mode and the mechanical mode. This effect may be considered as the insertion of *antidamping*, and therefore parametric instability will set in on attainment of some threshold value of the pump power.

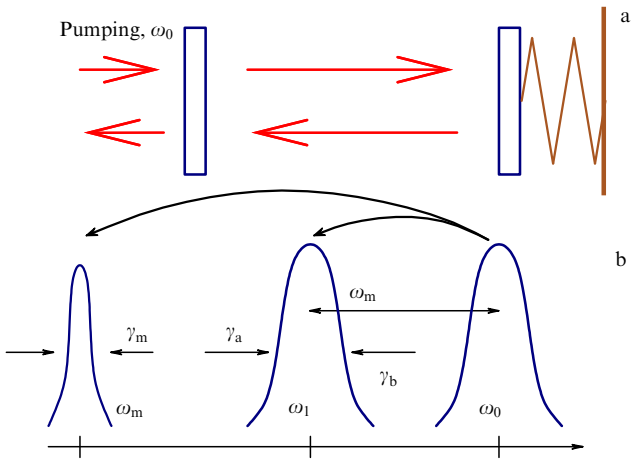

Figure 2. (a) Schematic of a Fabry–Perot resonator, one of its mirrors being mobile and a mechanical oscillator of frequency ω_m. (b) Mode diagram. The arrows indicate energy fluxes emerging in accordance with Manley–Rowe relations.

POI represents a threshold effect, its onset condition being conveniently described by factor $\mathcal{R}$:

$$\mathcal{R} = \frac{W\omega_1}{cLm\omega_m\gamma_1\gamma_m}\,\frac{\Lambda}{1 + (\Delta_1/\gamma_1)^2} > 1\,, \tag{3}$$

$$\Delta_1 = \omega_0 - \omega_1 - \omega_m\,, \tag{4}$$

$$\Lambda = \frac{V_m \left| \int \mathcal{A}_{0in}\mathcal{A}^*_{1in} u_\perp \, \mathrm{d}\mathbf{r}_\perp \right|^2}{\int \left|\mathcal{A}_{0in}(\mathbf{r}_\perp)\right|^2 \mathrm{d}\mathbf{r}_\perp \int \left|\mathcal{A}_{1in}(\mathbf{r}_\perp)\right|^2 \mathrm{d}\mathbf{r}_\perp \int \left|\mathbf{u}(\mathbf{r})\right|^2 \mathrm{d}\mathbf{r}}\,, \tag{5}$$

where W is the power circulating in the fundamental mode of the Fabry–Perot resonator, γ_1 and γ_m are the damping coefficients of the optical Stokes and elastic modes, L is the distance between Fabry–Perot resonator mirrors, c is the speed of light, m is the mirror mass, Δ_1 is the frequency mismatch, Λ is the overlap factor for the optical fundamental, optical Stokes, and elastic mode distributions, $\mathcal{A}_0$, $\mathcal{A}_1$ are the light field distribution functions over the beam section for the fundamental and Stokes modes, $u_\perp$ is the component of the elastic-mode displacement vector $\mathbf{u}$ perpendicular to the mirror surface, $\mathrm{d}\mathbf{r}_\perp$ corresponds to integration over the surface area of the mirror, and $\mathrm{d}\mathbf{r}$ corresponds to integration over the mirror volume V_m.

When parametric instability condition (3) is fulfilled, the energy $\mathcal{E}_0$ in the fundamental mode at the ω_0 frequency ceases to increase on a further rise in laser pump power W, while the energies of the Stokes and mechanical modes begin to grow [11] (Fig. 3). This growth may have the effect that the Stokes mode will serve as the pump for the excitation of the next appropriate pair of Stokes and mechanical modes. Thus, a cascade development of parametric instability becomes possible.

The POI phenomenon was observed in optical microcavities [12–14] for a modest optical pump power, on the order of 10^{-4} W; this is due to the high Q factors of optical modes (on the order of 10^9) and the small effective mass of mechanical oscillations (about 10^{-10} kg). It is relatively easy to obtain a cascade POI in these microcavities, which makes it possible to generate optical combs [15–18].

It should be emphasized that an appropriate optical *anti-Stokes* mode with a frequency $\omega_{1a} \simeq \omega_0 + \omega_m$ may also exist in the resonator. Then, in accordance with the Manley–Rowe relations, the pumping will insert *positive* damping into the mechanical mode, which may exceed the negative friction inserted by the Stokes mode and make parametric instability impossible [19]. In this case, a photon of the pump wave will be scattered by the elastic phonon to produce a photon of the anti-Stokes wave, while a part of the energy will be borrowed from the elastic wave. And so, on the one hand, the presence

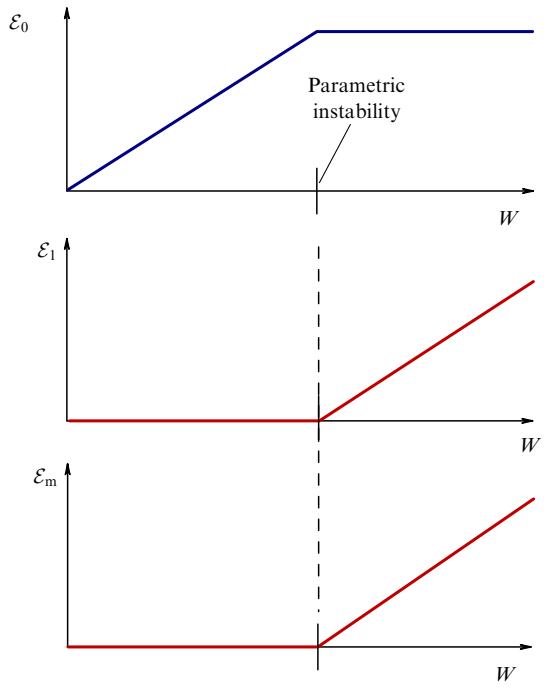

Figure 3. Respective energies $\mathcal{E}_0$, $\mathcal{E}_1$, and $\mathcal{E}_m$ of the fundamental, Stokes, and mechanical modes as functions of pump power W below and above the parametric instability threshold.

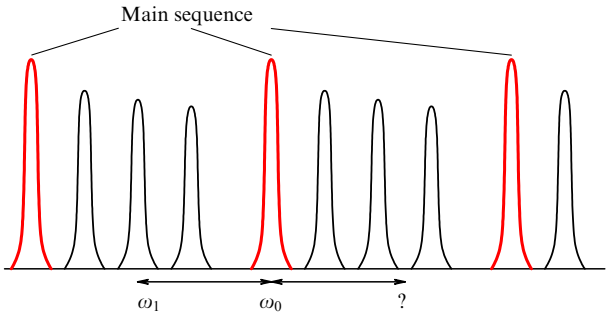

Figure 4. Structure of the optical modes of a Fabry–Perot resonator. The modes of the main sequence correspond to the high peaks. The optical Stokes mode has a frequency ω_1, and the possible anti-Stokes mode is indicated with a question mark.

of the optical Stokes mode is responsible for the insertion of antidamping into the mechanical mode (and therefore for the parametric instability effect), and, on the other hand, the presence of the anti-Stokes mode brings about the mechanical mode damping. However, the probability that the anti-Stokes mode suppresses the parametric instability completely is low enough, as illustrated by Fig. 4.

Parametric instability in laser interference antennas. To date, several laboratories in different countries have demonstrated the operation of first-generation gravitational wave detectors (the Laser Interferometer Gravitational Wave Observatory (LIGO) [20, 21], VIRGO [22], GEO-600 [23], and TAMA [24] projects), and efforts are underway by now to create second-generation detectors (Advanced LIGO (AdLIGO), Advanced VIRGO, GEO-HF, etc.), which will make it possible to detect gravitational waves in the near future. It is planned to substantially increase in the second-generation detectors the optical power circulating in the interferometer arms (up to 800 kW in AdLIGO). Therefore, the probability

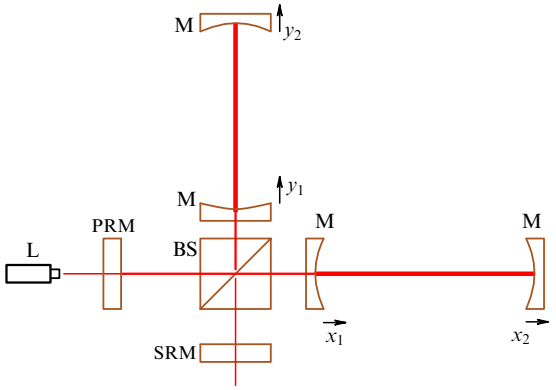

Figure 5. Simplified AdLIGO configuration: L — laser, BS — beam splitter, M — mirrors in the interferometer arms, PRM — power recycling mirror, SRM — signal recycling mirror. The light passing through the dark port (through the SRM) carries information about the difference in length between the interferometer arms $[(x_2 - x_1) - (y_2 - y_1)]$.

of developing POI in the second-generation laser gravitational detectors will be high enough.

A simplified schematic representation of the AdLIGO interferometer is given in Fig. 5. Two cylindrically shaped mirrors suspended at a long distance (4 km) from each other make up the first Fabry–Perot resonator in one interferometer arm; two other mirrors, the same as the two first, make up another arm with the second Fabry–Perot resonator, which is perpendicular to the first one. The laser beam of a pump laser passes through a beam splitter located at the arms intersection point. The light is assumed to experience multiple reflections from the mirrors inside each of the arms prior to its return to the beam splitter. The interferometer arms are so aligned that all reflected light is directed back to the laser (the so-called bright port), but the light does not arrive at a detector port (the so-called dark port). Some difference in arm lengths appears under the action of a gravitational wave, and a part of the light travels to the dark port and is recorded by a photodetector. The AdLIGO is targeted to attain the parameter values collected in Table 1.

Table 1. Parameters of the AdLIGO interferometer.

Power	0.83×10^6 W
Arm length	4000 m
Mirror mass	40 kg
Mirror radius	0.17 m
Mirror height	0.2 m
Material	Fused silica

The influence exerted by a gravitational wave, which gives rise to the difference in arm lengths, is extremely small: the AdLIGO interferometer is supposed to measure a difference in displacements on the order of $10^{-17} - 10^{-16}$ cm in a time of $\sim 10^{-2}$ s for an arm length of 4 km. Detection of so small a displacement implies extremely small mirror displacements caused by other factors — thermal, seismic, and technical noise. Even minor mirror displacements alter the phases of the beams that arrive at the beam splitter, thereby simulating the detection of a gravitational wave.

To predict unstable mode combinations requires complete information both about elastic modes and about optical Stokes modes. The frequencies and optical field distributions over the mirror surfaces are easy to calculate analytically for the Gaussian modes of a Fabry–Perot resonator [25], while the frequencies and displacement vector distributions for elastic modes can be determined only by numerical techniques. (The superposition technique is employed in application only to the axially symmetric elastic modes of a cylindrical mirror [26].) One can see from condition (3) that the uncertainties in calculating the eigenfrequencies of elastic modes must be smaller than the value of the damping coefficient of the optical Stokes mode. For typical mechanical frequencies ranging from 10 kHz to 100 kHz and an optical relaxation time corresponding to a 10–100 Hz frequency interval, this signifies that the relative uncertainty of numerical calculations of elastic mode frequencies should be within 10^{-4}. This requirement is not always fulfilled in the calculation of elastic modes using, for instance, the COMSOL numerical code package. It is also noteworthy that the nonuniformities in the distribution of the density and Young modulus of the mirror material may give rise to an elastic mode frequency shift at a level of 10^{-3}. For instance, with the use of the ANSYS package to numerically solve grid problems, the accuracy of elastic mode calculations was about 0.5% [8–10, 27]. Therefore, the existing precision of elastic mode calculations is insufficiently high.

To this we can add the uncertainty introduced by the material inhomogeneity of the mirrors; for fused silica, for instance, the relative density variations are at a level of $\delta\rho/\rho \approx 10^{-3}$.

3. Conclusions

So, let us list the possible ways of avoiding parametric instability in second-generation laser gravitational antennas.

First, there is good reason to search for precursors, i.e., discover weak oscillations at Stokes and mechanical frequencies. This will permit inserting noiseless damping into the acoustic modes or change the spectrum of optical modes.

Second, since the theoretical and numerical analyses are insufficient, it is necessary to observe parametric instability in a real antenna. This will enable working out different techniques of suppressing the instability.

The third way is to lower the optical power circulating in interferometer arms: second-generation gravitational antennas are intended to attain the accuracy of the standard quantum limit [5] at frequencies of about 100 Hz. This frequency is determined by the high quality of isolation from seismic noise. It is significant that the requisite optical power is proportional to the *cube* of the frequency. If attempts to go over from the 100 Hz frequency to the 30 Hz frequency meet with success, the circulating power will become much lower: it would suffice to have about 20 kW instead of 800 kW. Furthermore, the gravitational radiation intensity is higher in a lower frequency range, according to predictions.

References

1. Migulin V *Tr. Fiz. Inst. Akad. Nauk SSSR* (3) 77 (1938)
2. Migulin V *Radiotekh. Elektron.* **5** 995 (1960)
3. Migulin V *Vestn. Mosk. Univ. Ser. 3* (6) 67 (1960)
4. Migulin V V et al. *Osnovy Teorii Kolebanii* (Basic Theory of Oscillation) (Moscow: Nauka, 1978) [Translated into English (Moscow: Mir, 1983)]
5. Braginsky V B *Fizicheskie Eksperimenty s Probnymi Telami* (Physical Experiments with Probe Bodies) (Moscow: Nauka, 1970)
6. Braginsky V B, Strigin S E, Vyatchanin S P *Phys. Lett. A* **287** 331 (2001)
7. Braginsky V B, Strigin S E, Vyatchanin S P *Phys. Lett. A* **305** 111 (2002)
8. Zhao C et al. *Phys. Rev. Lett.* **94** 121102 (2005)
9. Ju L et al. *Phys. Lett. A* **355** 419 (2006)
10. Ju L et al. *Phys. Lett. A* **354** 360 (2006)
11. Polyakov I A, Vyatchanin S P *Phys. Lett. A* **368** 423 (2007)
12. Kippenberg T J et al. *Phys. Rev. Lett.* **95** 033901 (2005)
13. Matsko A B et al. *Phys. Rev. A* **71** 033804 (2005)
14. Rokhsari H et al. *Opt. Express* **13** 5293 (2005)
15. Savchenkov A A et al. *Phys. Rev. Lett.* **101** 093902 (2008)
16. Grudinin I S, Yu N, Lute M *Opt. Lett.* **34** 878 (2009)
17. Del'Haye P et al. *Nature Photon.* **3** 529 (2009)
18. Kippenberg T J, Holzwarth R, Diddams S A *Science* **332** 555 (2011)
19. Kells W, D'Ambrosio E *Phys. Lett. A* **299** 326 (2002)
20. Abramovici A et al. *Science* **256** 325 (1992)
21. Sigg D et al. (for the LIGO Scientific Collab.) *Class. Quantum Grav.* **25** 114041 (2008)
22. Acernese F et al. *Class. Quantum Grav.* **25** 114045 (2008)
23. Grote H (for the LIGO Scientific Collab.) *Class. Quantum Grav.* **25** 114043 (2008)
24. Takahashi R et al. (TAMA Collab.) *Class. Quantum Grav.* **25** 114036 (2008)
25. Kogelnik H, Li T *Appl. Opt.* **5** 1550 (1966)
26. Meleshko V V, Strigin S E, Yakymenko M S *Phys. Lett. A* **373** 3701 (2009)
27. Gras S, Blair D G, Zhao C *Class. Quantum Grav.* **26** 135012 (2009)

PACS numbers: 91.25.Mf, **94.30.–d**, **96.60.–j**
DOI: 10.3367/UFNe.0182.201203h.0327

Solar-terrestrial physics and its applications

V D Kuznetsov

1. Introduction

The N V Pushkov Institute of Terrestrial Magnetism, Ionosphere and Radio Wave Propagation of the RAS (IZMIRAN in *Russ. abbr.*), which Vladimir Vasil'evich Migulin led for nearly 20 years (from 1969 to 1988), is a multidisciplinary institute. It embraces different realms of physics: astronomy and astrophysics, geophysics, radiophysics and plasma physics, nuclear physics, etc. Solar–terrestrial physics, which studies processes in the Sun–Earth system, is one of IZMIRAN's main lines of inquiry. V V Migulin, as IZMIRAN's Director and Chair of the Scientific Council on the Problem of Solar–Terrestrial Relations of the RAS (the Sun–Earth Council), for many years was involved in solar–terrestrial physics and supervised a number of programs and projects.

Along with investigations into basic phenomena and processes in the Sun–Earth system, the solar–terrestrial physics of our days has many practical applications related

V D Kuznetsov N V Pushkov Institute of Terrestrial Magnetism, Ionosphere and Radio Wave Propagation, Russian Academy of Sciences, Troitsk, Moscow region, Russian Federation. E-mail: kvd@izmiran.ru

Uspekhi Fizicheskikh Nauk **182** (3) 327 – 336 (2012)
DOI: 10.3367/UFNr.0182.201203h.0327
Translated by E N Ragozin; edited by A Radzig

to different areas of human activity [1]. In recent years, a broader term is used to denote this realm of research — heliophysics [2], as has been recognized that Earth and terrestrial processes are affected not only by the phenomena occurring on the Sun, but also by numerous processes proceeding in the heliosphere — the vast domain around the Sun filled with solar wind.

To understand the processes occurring in the Sun–Earth system, first and foremost it should be realized how the Sun is structured and how it operates, and what the space environment of Earth is and how it changes.

2. Solar model — from the core to the heliopause

The modern model of the Sun comprises a dense core (~ 160 g cm^{-3}) about a quarter of the solar radius in size, which is the seat of thermonuclear reactions and their related energy release. This energy, in the form of radiation, is transferred through a radiation zone to the outer layers. In the outer layers, at a central distance slightly longer than two thirds of the solar radius, a convective zone forms, in which the heat removal outside from the inner layers by way of plasma motion is more efficient than by radiative heat transfer. Next come the layers of the outer solar atmosphere — the thin photosphere, which we see with the naked eye, the chromosphere, a transition region, and the corona, which passes into the solar wind forming the heliosphere (Fig. 1).

Information about the processes occurring in the solar core is obtained from ground-based neutrino measurements [3]. Helioseismology techniques permit modeling the structure and dynamics of the inner layers from surface observations of global solar oscillations [4]. Interior solar rotation is differential: the rate of rotation is depth- and latitude-dependent (Fig. 2), the near-equatorial zones rotate faster than the high-latitude ones, and the rate of rotation increases with depth. The dashed line in Fig. 2 marks the so-called tachoclinal layer in which the angular velocity exhibits a sharp jump, i.e., the motions are shear-like. It is precisely this region, especially where the angular velocity gradients are strongest, that is considered to be the principal element of the solar dynamo and the main generator of the magnetic field.

The differentiated character of solar rotation manifests itself in the equatorial plasma, together with its frozen magnetic field, moving faster than at high latitudes. As a result, a toroidal magnetic field forms from the poloidal solar field in the convective zone, with the former becoming stronger and, at some point in time, emerging from the convective zone to the solar surface due to the magnetic buoyancy effect and forming domains of a strong magnetic field there — sunspots and active regions, which give rise to different sporadic phenomena in the outer solar atmosphere.

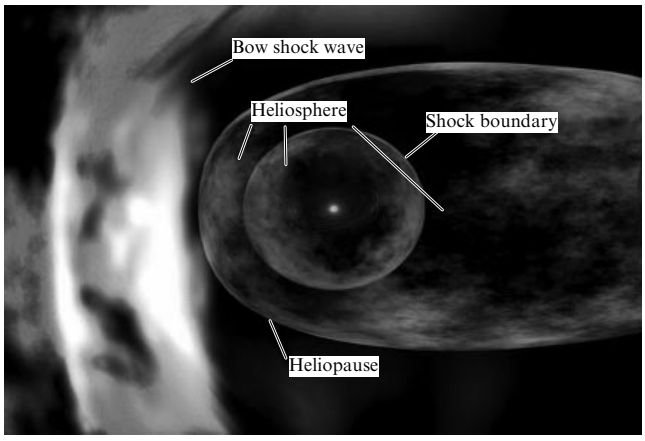

Figure 1. Heliosphere — region from the Sun to the heliopause (the boundary with the interstellar medium). [Processed image from NASA's site (see http://ru.wikipedia.org/wiki).]

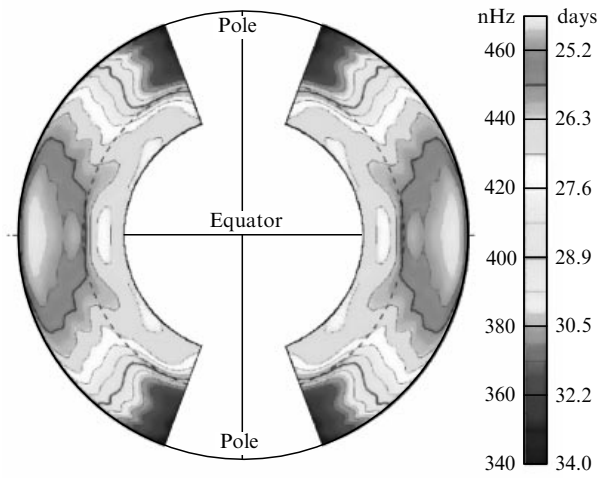

Figure 2. Profile of the angular velocity of the differentiated rotation in the cross section of the convective zone [5].

A sunspot is the egress of a magnetic flux tube to the surface of a photosphere, in which the field strength may range up to 4000 G. This strong field suppresses convection which brings heat from below, and therefore the area of magnetic flux tube egress to the photospheric surface appears darker than the surrounding hot photosphere, thereby justifying the very name 'spot'. The spot temperature is approximately 1000 °C lower than the ambient one (4500 °C), and such a spot on the photosphere is an indication of strong magnetic fields which are generated, are transported, decay, and dissipate during the solar cycle.

Observed in recent years, beginning from 1996 (the 23rd and 24th solar cycles), is a lowering of the spot field strength (Fig. 3) with an average rate of about 50 G per year [6]. Extrapolation of this tendency suggests that solar spot activity will disappear by the end of the current decade, i.e., by 2020. This is regarded as an anomaly in solar behavior and is associated with related anomalies on Earth (fall in temperature, etc.) by analogy with those observed in the past, as discussed in Section 3. When the field strength in the spots lowers to 1500 G, they become invisible on the photosphere and the possibility of using the spots to monitor the dynamics of magnetic fields in the 11-year solar cycle vanishes. The issue of whether the solar cycle itself is retained in this case remains an open question. It is not unlikely that during the Maunder solar minimum (1640–1710) the situation on the Sun was such that sunspots were invisible, while the cycle itself continued, and when the magnetic field in the spots rose again, they became visible and the spot-based observations of the cycles resumed and have continued up to the present time.

The observed lowering of magnetic field strength in sunspots, as discussed above, favors the hypothesis that the Sun may be entering a period of a Maunder-like minimum.

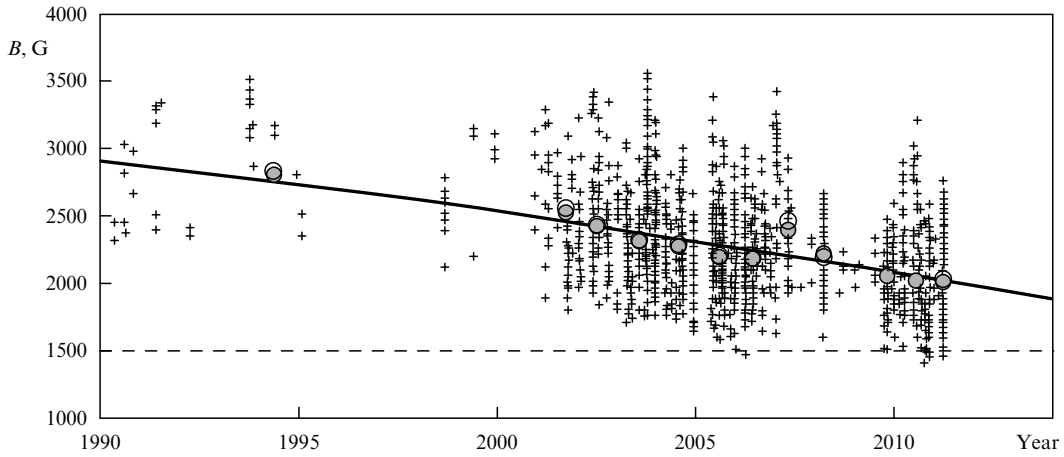

Figure 3. Lowering of a magnetic field strength in sunspots with time, according to Penn and Livingston [6].

The reason for this phenomenon has not been elucidated, and the answer to this question is to be searched for in the dynamo process of magnetic field generation. A question also arises here concerning the magnetic flux component in the solar cycle, which is contained in invisible spots with a low magnetic field strength: how many such spots are there, and what is the magnitude of this flux?

2.1 Flares and ejections

The emergence of magnetic fields from under the photosphere to the surface of the Sun gives rise to topologically complex magnetic configurations in its atmosphere. They are deformed by unceasing convective motions on the photosphere, generate high currents in the plasma atmosphere, and eventually become unstable to give birth to numerous active phenomena which are nonthermal in nature and are characterized by nonstationary plasma processes, particle acceleration, different kinds of radiation, etc.

Among the most powerful manifestations of sporadic solar activity are flares and mass ejections which possess the highest geoefficiency from the standpoint of their terrestrial effect. Today, the main problem in the study of solar flares and mass ejections reduces to understanding their trigger mechanisms [7]. We are unable to predict them, and this is one of the problems of solar–terrestrial physics, which may be solved on the basis of more thorough observations of magnetic field variations in active regions and on the basis of permanently refined models. Back in 1979, V V Migulin, jointly with M M Molodenskii and S I Syrovatskii, proposed an approach to the solution of this problem relying on Syrovatskii's theory of current sheets [8]. To date, this theory has been amply borne out by observational data, and it is not unlikely that this theory will underlie the methods for predicting solar flares.

2.2 Solar cycle

As is commonly known, the Sun experiences an 11-year solar cycle which involves a time variation of the number of sunspots. Although the cycle is referred to as an 11-year cycle, its period ranges from 8–9 to 13–14 years. Also varying is the amplitude of the solar cycles — the average relative number of sunspots at the peak of the cycle. The explanation of the solar cycle is underlain by the quasiperiodic action of magnetohydrodynamic dynamo process in the convective solar zone; however, so far we cannot predict with confidence forthcoming cycles — their duration, amplitude, and other characteristics.

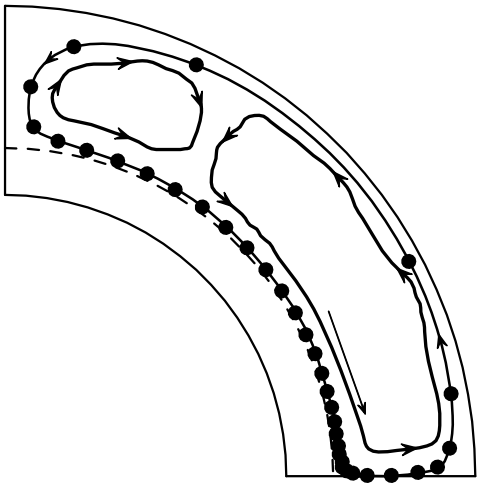

Figure 4. Decay of a meridional circulation vortex as one of the hypotheses explaining variations of the duration and amplitude of 11-year solar cycles.

One hypothesis for the cause of variations in the solar cycle period and the amplitude is associated with separation of the meridian circulation vortex in the convective zone into two vortices (Fig. 4), which changes the circulation time of the major vortex. Another hypothesis relies on the nonlinear character of the dynamo process — on the influence of the magnetic field on the motions, resulting in field enhancement [9]. The Intergelioprobe solar space project [10] now under development is drawn up for carrying out observations of the subpolar regions of the Sun and studying in greater detail the interplay between magnetic fields and plasma motions.

From ground-based measurements it was recently revealed that zonal flows (in the east–west direction) inside the Sun, or so-called torsion vibrations experiencing regular latitudinal changes, are associated with the solar cycle [11]. The origin of such variable zonal flows, which come from the depths of the convective zone, has not been elucidated. The latitude at which this zonal flow shows up defines the latitude of new sunspot formation in each cycle. Observations of these flows made it possible to successfully predict the delay of the onset of the current, 24th, solar cycle (2008–2019), which took

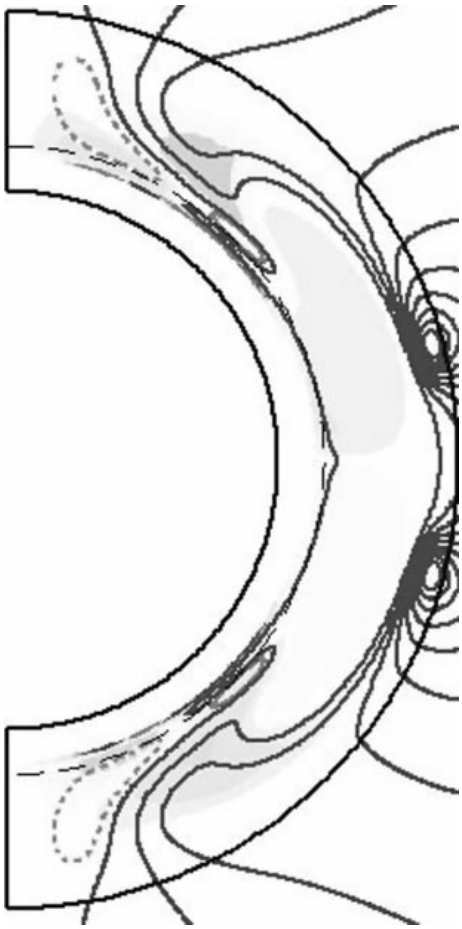

Figure 5. Change of sign of the magnetic field in polar solar zones in the solar cycle as a result of magnetic field transfer from the equator to the poles [14] (the solid and dashed lines correspond to the magnetic fields of different signs).

place because of weakening of these flows. It had been expected that in 2011 it would be possible to see the onset of the zonal flow responsible for the next, 25th, cycle, but manifestations of this flow have not been discovered so far. This is an indication that the 25th cycle may commence in 2021–2022 (rather than in 2019) or not commence at all [12].

The transfer of decaying magnetic fields normally occurs in a solar cycle towards solar poles at which the poloidal field changes sign (Fig. 5). Observations over the past 40 years [13] have revealed a moderation of this transfer, and no such poleward transfer is taking place at present, maybe because of the later onset of the 24th cycle and its slow development. If the current 24th cycle, which remains weak, fails to restore this transfer and replace the magnetic field of the 23rd cycle by a field of opposite sign, as is usually the case, it will be difficult to predict the impact of the dynamo process and the behavior of the Sun in this situation.

2.3 Solar wind and the heliosphere

Solar wind — a charged particle flux — continuously emanates from the Sun. The solar wind flows around the terrestrial magnetosphere and is the source of geomagnetic disturbances. So-called coronal holes are produced on the Sun, which are seen as dark coronal regions. They are the domains of open lines of force, which emanate the high-velocity solar wind. When Earth finds itself in the interplanetary magnetic field sector corresponding to a solar coronal hole, magnetic storms occur on Earth. The solar poles emanate the fast solar wind (~ 800 km s^{-1}), and the equatorial plane emanates the slow one (~ 400 km s^{-1}). Near-polar coronal holes with the fast solar wind sometimes sink to the plane of the ecliptic, and Earth finds itself in the sector of these high-velocity streams, which is attended by an enhancement of geomagnetic activity.

Figure 6. Corrugated and helically swirled heliospheric current sheet ('ballerina's skirt') and Earth's motion around the Sun (after T Hoeksema).

The sources of solar wind on the Sun are unknown. It is hypothesized that it emanates from the boundaries of the chromospheric network. The substance in a convective cell rises upwards at its center and is transferred to the edges together with the magnetic fields, where small magnetic loops reconnect with the loops of another cell, and field dissipation and plasma heating emerge with the result that the plasma pressure, together with magnetic forces, 'blow out' the substance upwards. The solar wind is formed just from these streams. This hypothesis will be tested in the Intergelioprobe project in observations of the Sun with a high spatial resolution at close range [10].

Owing to the rotation of the Sun, the interplanetary magnetic field (IMF) is structurally spiral (Fig. 6). The inclination of the magnetic solar axis with respect to the ecliptic plane ($\sim 7^\circ$) and the existence of active regions on the solar surface have the consequence that the heliospheric current sheet, which separates the magnetic fields of opposite polarities, possesses, apart from a spiral structure, a corrugated structure in the form of a ballerina's skirt. Earth crosses the corrugated structure of the heliospheric current sheet in its orbital motion; the sign of the IMF changes in this crossing, as does the character of the interaction between the IMF and the terrestrial magnetic field.

At a distance of about 100 A.U., the solar wind pressure becomes equal to the pressure of the interstellar medium, and a boundary of the Solar System is formed, which is termed the heliopause (a contact surface) (see Fig. 1). Since both the solar wind and the incident flow of the interstellar medium (owing to the rotation of the Sun about the Galaxy center) are supersonic, their collision gives rise to two shock waves on opposite sides of the heliopause. This complicated and rather lengthy structure separates the Solar System from the galactic medium. The heliosphere changes in dimension according to the power of the solar cycle and the solar wind pressure head.

In the foregoing, we considered the main physical objects of heliophysics, and now we turn to solar–terrestrial physics itself, bearing in mind the impact of solar activity on Earth and its related applications.

3. Applications of solar-terrestrial physics

The main agents of solar activity — flares, mass ejections, and the solar wind — are the sources of space weather which is considered today as an integral part of the human environment and the scope of human activity [15]. Solar activity perturbs the heliosphere and the circumterrestrial space, giving rise to a wealth of solar-driven effects on Earth. These effects, which take place in the magnetosphere, atmosphere, and ionosphere of Earth, as well as on its surface, affect the human environment and activity on Earth and in space.

The magnetic field of the Earth protects us from the hazardous effects of solar activity — accelerated charged particle streams, the solar wind, and the highest-power manifestations of solar activity — solar mass ejections. Earth's magnetosphere elongates under the action of the solar wind in the direction away from the Sun (Fig. 7) and a magnetospheric tail forms on the night side, while the day side region of the magnetosphere contracts.

The internal volume structure of the magnetosphere is rather complicated: it contains a magnetopause (a boundary with the solar wind), a plasmasphere, current systems, and cusps. The day (frontal) side of the magnetosphere is pressed by the solar wind head; here, the boundary magnetospheric point is located at approximately 10 terrestrial radii, while the night (extended) tail of the magnetosphere is traced at distances greater than 100 terrestrial radii.

Solar mass ejections and solar wind fluxes travel from the Sun through the interplanetary medium and collide with the terrestrial magnetosphere to give birth to magnetic storms. When the solar wind and the mass ejections interact with the terrestrial magnetosphere, the reconnection of magnetic lines of force in its tail, the capture of particles, and their precipitation in magnetic polar regions with the formation of auroral oval occur, which results from high-energy particle precipitation into the atmosphere and the glow of excited atmospheric atoms.

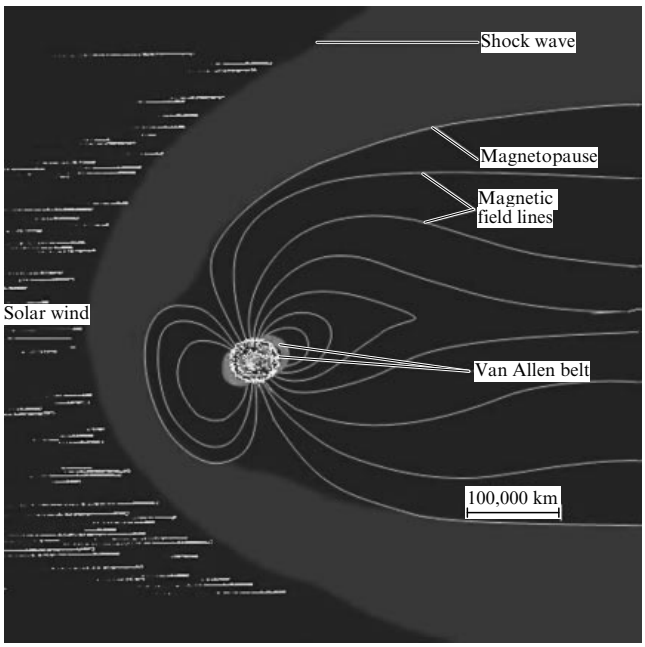

Figure 7. Structure of the Earth's magnetosphere formed when the solar wind flows around it.

The geomagnetic disturbances are most pronounced near the magnetic poles in the region of the auroral oval and in the neighboring territories. The zone of strong geomagnetic disturbances usually covers the northern regions of Russia, North America, and Scandinavia. During the very strong solar events in October–November 2003, the auroras could be seen in Moscow and even from the latitude of Odessa, whence it follows that strong geomagnetic disturbances cover a substantial part of the territory of the terrestrial globe.

The maximum number of magnetic storms is observed near the peak of the solar cycle, with a small shift to the right from the cycle's peak.

Let us consider examples and mechanisms of the action of solar activity factors on the fields of human activity on Earth and in space.

During a magnetic storm, one of the effects is underlain by the Faraday law of electromagnetic induction. Variations of the terrestrial magnetic field during a magnetic storm give rise to a vortical electric field which penetrates the entire space, and when there is a closed conductive circuit an electromotive force and an electric current are generated in it [16]. The vortical electric field manifests itself during magnetic storms in the form of a short pulse several seconds long. The potential difference therewith is equal to about 2–3 V km^{-1}, so that a voltage of 220 V appears across the ends of a 70–110-km-long conductor. During magnetic storms, the global vortical electric field penetrates in the first several seconds all circumterrestrial space, the atmosphere, and Earth itself.

As a result, so-called geomagnetically induced currents emerge during magnetic storms in all conducting systems, both natural (Earth, ocean, atmosphere, ionosphere, magnetosphere) and technical (long-distance power transmission lines, communication lines, oil and gas pipelines, railroad metals, power supply lines, etc.), which are the most dangerous factor from the standpoint of affecting the operation of the parts of the energy infrastructure listed above [17]. The greater the spatial scale of the power system, the higher the induction current, and the stronger the disturbance effect.

In the substations of power transmission lines, the geomagnetically induced currents flow through the earth via transformer windings and ground connections, i.e., where there are no protective relay devices, and herein lies the danger. In energy systems, these currents lead to dangerous effects, like the saturation of transformers and their overheating and disruption, the generation of parasitic current harmonics, and the failure of protective relays and the consequential tripping of power transmission lines.

The most serious consequence of a strong magnetic storm was the energy disaster of 13–14 March 1989 in the province of Quebec, Canada, when a powerful auroral oval covered the entire territory of North America, northern Europe, and the northern regions of Russia, with the result that the entire province, plus Canada's capital Ottawa, experienced a blackout for nine hours [18].

Let us consider briefly the sequence of events in the Sun–Earth system which led to that disaster.

From the 5th to the 19th of March 1989, an active region moved over the solar disk and crossed the central meridian on

March 12. During that period, the active region produced 11 X-ray flares, 4 of which were large. These flares were attended by mass ejections in the form of plasma clouds. The ejections of March 9 and 10 were directed towards Earth. The arrival of shocks and ejections on Earth was recorded in the form of sudden jumps in magnetic field records on March 13. The shocks traversed the path from the Sun to Earth in 82 and 61 h, respectively, which corresponds to propagation velocities of about 500–700 km s^{-1} through the interplanetary medium.

During the development of the magnetic storm, the stationary compensators of alternating current shut down in the Quebec power system, which led to the tripping of power transmission lines; as this took place, transformers were damaged by voltage overload, and eventually the entire energy system experienced blackout.

Transformers fused not only in Quebec, but also in the USA, Europe, and Great Britain due to overheating, and a blackout occurred. One of the most dangerous moments of this disaster was the failure of a step-up transformer in an atomic plant in New Jersey, which fortunately did not result in another disaster but caused major damage and led to the appreciation and understanding of the reality and the large scale of space weather hazards.

The solar event of 1 September 1859 — the so-called Carrington event [19] — is considered to be the highest in power over the whole period of observations. In this case, the disturbance from a high-power solar flare reached Earth in a record short time (17.5 h) and produced an extremely strong magnetic storm. Serious telegraph communication disturbances were recorded in the United States and Europe, which continued for several hours. At night, the auroras were observed wherever they had never been observed before: in Rome, Havana, Hawaii, and even near the equator. Should an event of this power, which was several times higher than the power of the Quebec event, occur today, in the era of society's advanced technical infrastructure, it would have much more severe consequences according to experts' estimates than those of the Quebec event [20]. Therefore, Nature has already warned us that the development of technical systems has reached a level whereby the actions of space weather factors on them may lead to serious disasters [21].

Geomagnetical currents induced during magnetic storms, which are regularly recorded in the power circuits in North America and northern Europe, result in power system abnormalities which pose threats related to economic damage, industrial safety issues, and many other aspects of life.

Oil and gas pipelines are also vulnerable to the action of geomagnetically induced currents [22]. An example is provided by the regular recording of such currents in the Alaska pipeline, where they range up to several hundred amperes in magnitude. The geomagnetically induced currents in pipelines change the electrical potential of the pipe and thereby disrupt the operation of corrosion prevention systems. Where the potential is above the critical one, localized corrosion spots make their appearance on the pipe, resulting in a shorter lifetime of the pipeline. This lifetime is estimated at 20–40 years, while corrosion spots attributed to the effect of geomagnetically induced currents appear within three years of service.

On the Northern Railroad in the Arkhangel'sk region, from time to time malfunctions occur in the operation of railroad transport electronics, which are caused by geomagnetic activity and geomagnetically induced currents in power transmission lines and rails, and which are responsible for failures in the operation of traffic lights. Similar malfunctions occur in other parts of the railroad. Systematic work and execution of a special program (exploratory and technical) are required in this case to develop protective systems.

Magnetic storms result in the swelling of the terrestrial atmosphere: dense layers of the atmosphere rise upwards to cause abnormal deceleration of the International Space Station (ISS) and satellites. This necessitates raising their orbits and delivering fuel to the ISS, requiring additional time and expenses. During the 1989 Quebec event, the American satellite positioning system was paralyzed, because the satellite orbit parameters changed owing to the anomalous deceleration, and some of the satellites were lost. In the 1970s, the American orbital Skylab station deorbited uncontrollably, because the factors of enhanced solar activity responsible for atmospheric swelling were not taken into account in the calculation of Skylab's orbital lifetime.

Space infrastructure is seriously endangered. The electromagnetic and corpuscular radiation of solar flares exerts a variety of adverse effects. First and foremost is the radiation hazard to astronauts and to satellite electronics. The terrestrial magnetic field acts as a shield which prevents high-energy solar particles from penetrating deep into the magnetosphere. So-called radiation belts, the outer and the inner ones are formed inside the magnetosphere; during magnetic storms, they deliver radiation quanta to the ionosphere and the atmosphere and thereby produce a radiation hazard. The far ultraviolet radiation and X-rays of solar flares change the ionization of the ionosphere and disturb radio communications.

About 37,000 solar flares occur during a solar cycle. Earth experiences more than 600 magnetic storms, 10 of which are very strong and one extremely strong and capable of leading to a disaster like the Quebec one.

Important in many respects is the question of the sign reversal of the terrestrial magnetic field [23, 24]. This is a very rare phenomenon occurring over long periods of time, which consists in the north and south magnetic poles of Earth changing places (as if the magnetic dipole flips). It is hypothesized that the last sign reversal occurred about 780 thousand years ago. In the past, the sign reversals took place irregularly, with intervals ranging from several thousand to several hundred years. Since there are magnetic anomalies unrelated to deep sources of the dipole geomagnetic field, the field in the sign reversal does not vanish completely, with the sign reversal of the magnetic field proceeding slowly and nonuniformly over the planet.

For last 400 years, the magnetic field intensity of the Earth dipole has been observed to be weakening [25]: over this period it has lowered by about 20%. To a certain extent, this is regarded as a trend towards the sign reversal of the geomagnetic field. Figure 8 demonstrates the motion of the south magnetic pole (located on the north geographic pole, this 'south' magnetic pole is commonly known as the North Pole) over the last approximately 200 years, which was measured in the past (i.e., the actual motion), calculated following a model for the present period, and theoretically predicted for the future.

Proceeding from the analysis of the recent motion of magnetic poles [27], it was determined that the previously observed accelerated motion of the north magnetic pole terminated in about 2003 on attaining a velocity value of

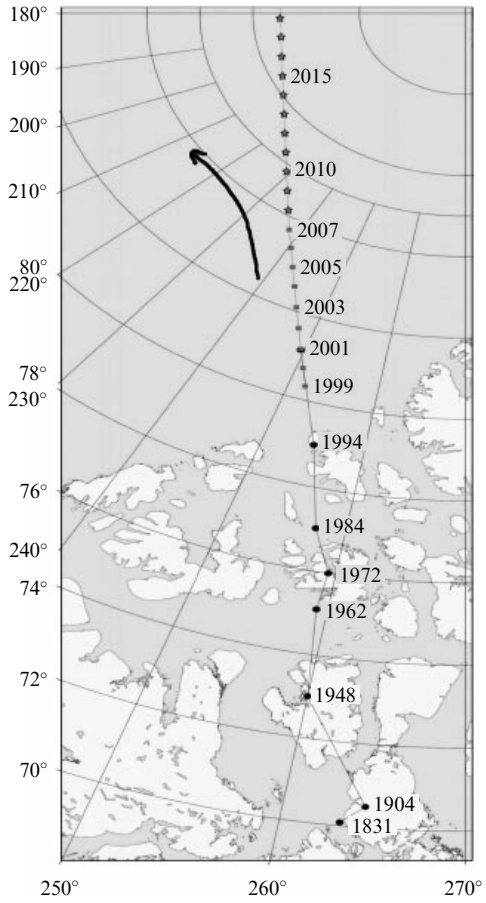

Figure 8. Motion of the position of the terrestrial magnetic pole over the past centuries [26]. The arrow shows the deflection of the real pole's motion from the previously predicted one.

approximately 62.5 km per year. Then the pole motion began to slow down, and its velocity in 2009 lowered to about 45 km per year. In this case, the pole started turning slightly towards Canada, while moving in the northwest direction as before. Specifically, the latitudinal velocity lowered from 58 to 35 km per year during the period under investigation (2001–2009), while the longitudinal velocity increased from 23 to 32 km per year. This gives reason to believe that the magnetic pole simply 'wanders', will not leave the region of the Canadian anomaly, and will not reach Siberia in about 50 years, as predicted earlier.

Air flights across the North Pole are expedient from the standpoint of shortening distances; however, they pass through the auroral oval, and a risk is run that the crew and the passengers will experience a higher radiation dose during a magnetic storm. Furthermore, radio communications with the plane are disturbed in this case. Flying around the pole signifies an increase in distance, time, fuel consumption, and expenses. Predictions of the state of solar and geomagnetic activity are required here to avoid extraordinary situations.

The action of accelerated solar protons, which were produced in an extreme solar event, on the European–American SOHO (SOlar and Heliospheric Observatory) satellite is exemplified by Fig. 9; the satellite was beyond the Earth's magnetosphere and was not protected by it. The particles found their way into detectors and the satellite became 'blind' — the solar image was covered with 'snow'. For comparison, at that time the CORONAS-F satellite

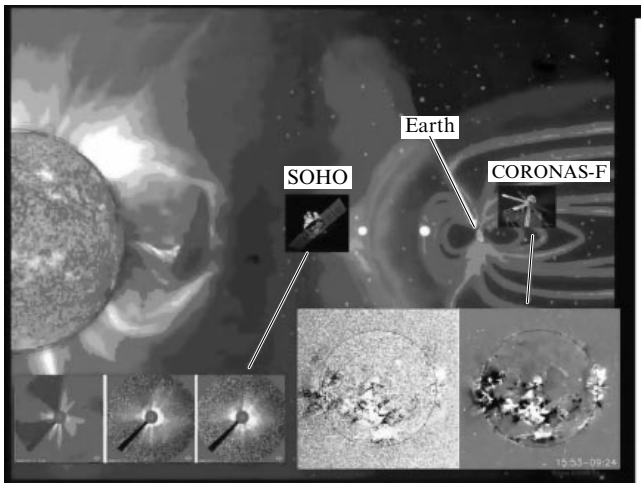

Figure 9. Effect of protons accelerated in solar flares on the SOHO spacecraft telescopes located beyond Earth's magnetosphere.

[CORONAS is an acronym of the Russian-language Kompleksnye ORbital'nye Okolozemnye Nablyudeniya Aktivnosti Solntsa (Complex Orbital Near-Earth Observations of the Sun Activity)] was positioned within the magnetosphere and was able to obtain high-quality images of that extreme event. The bright point at the left of Fig. 9 is the frontal point of the magnetosphere, which is usually located at a distance of ten terrestrial radii from Earth. During the emergence of high-power solar wind fluxes and solar mass ejections, this distance may shorten to five terrestrial radii, so that all geostationary satellites (the bright point on the right side of the drawing at a distance of six terrestrial radii), which afford mobile communications and television, find themselves in open space and are in no way protected from solar radiation. In this instance, too, online and short-term predictions of space weather are required as a constituent of the system of precautions to ensure the safe operation of space vehicles.

Intense microwave radiation (with frequencies of about 10 GHz) from solar flares 'jams' the measuring channels of certain satellites, resulting in a loss of space data transmitted to ground-based receiving centers. The radio emission passes through the ionosphere and reflects from the ocean in all directions to arrive at the receivers and transmitters of the satellites [28].

When disturbed during a magnetic storm, the ionosphere scatters the navigation GPS (Global Positioning System)/GLONASS (GLObal NAvigation Satellite System) signal, leading to errors in object positioning. In a heavy fog, military planes land on the deck of an aircraft carrier using the GPS navigation signal, which is accurate to within 1 m. During magnetic storms, in some regions of the terrestrial globe this accuracy may lower to 100 m.

Accelerated protons from large solar flares are responsible for a lowering of the content of the upper ozone layer in the polar middle mesosphere, destroying up to 70% of the ozone molecules over a period from a week to a month [29]. Forecasting the time intervals of such ecologically important phenomena is directly related to forecasts of proton solar flares.

An association between the moments Earth crossed the boundaries of the sector structure of the interplanetary magnetic field (IMF) (see Fig. 6) and a variation of vorticity in the upper terrestrial atmosphere and the origin of

extratropical cyclones has been established [30]. This effect, which was discovered back in the 1970s, was recently verified anew and has been amply borne out on the basis of new data [31]. If a satellite equipped with a magnetometer is placed ahead of Earth in its orbital motion around the Sun in order to record the impending crossings of the boundaries of the sector structure of the IMF and its sign reversal, it will be possible to monitor the state of atmospheric vorticity and the related origin of extratropical cyclones.

All available knowledge and data about the processes in the Sun–Earth system are used for forecasting space weather. The most powerful space weather prediction center is at the National Aeronautics and Space Administration (NASA). The IZMIRAN Space Weather Forecasting Center (see http://forecast.izmiran.ru) produces daily information about the state of space weather and the geomagnetic situation, which is broadcast and transmitted to the Ministry of the Russian Federation for Civil Defense, Emergencies and the Elimination of Consequences of Natural Disasters, the Russian Federal Space Agency (Roscosmos), the Mission Control Center, and other organizations for operational management to ensure the safe functioning of the corresponding infrastructure. These forecastings are in demand today.

3.1 Solar activity and climate

A few words are in order on the influence of solar activity on the climate of Earth. Studies of this problem make up a separate area which covers different aspects of solar–terrestrial physics, the physics of the atmosphere and hydrosphere, geophysics, etc. The solar constant (1367 W m^{-2}) — the amount of solar energy incident on the upper atmosphere of Earth — is hardly changed with the solar cycle; its variations, which are on the order of 0.1%, cannot produce noticeable climatic changes. Meanwhile, the amount of solar energy absorbed by and reflected from Earth may vary with the state of the terrestrial atmosphere, and herein lies the crux of the problem.

Among the variety of factors affecting the climate, the emphasis in solar–terrestrial physics is placed on the influence of cloudiness [32], which is modulated with galactic cosmic rays (GCRs). Their penetration into the Solar System and the atmosphere of Earth is, in turn, modulated with solar activity (the solar cycle) — the magnetic field of the Sun and the solar wind (Fig. 10). Enhanced solar wind fluxes at the peak of the solar cycle mitigate (sweep out) the GCR fluxes from the Solar System. Galactic cosmic rays can produce aerogels in the terrestrial atmosphere and stimulate the formation of cloud cover, thereby changing Earth's albedo and the passage of solar radiation fluxes to the terrestrial surface.

From data collected over many years (about 1000 years) it was determined that there is a correlation between the temperature on Earth and the level of solar activity determined by the content of C^{14} isotope (Fig. 11). The higher the level of solar activity, the lower the intensity of GCRs, the lighter the cloudiness, and the greater the amount

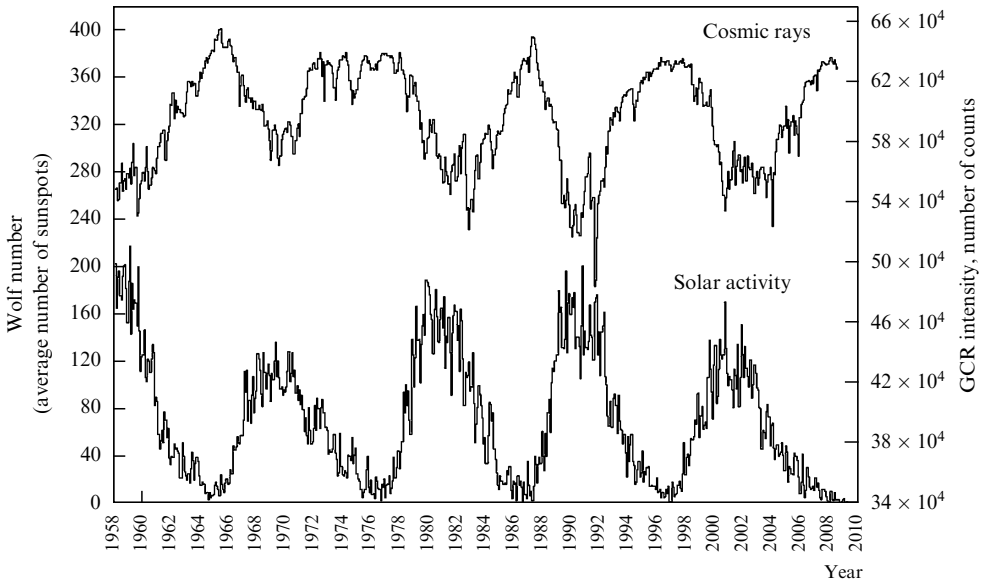

Figure 10. Correlation between the enhanced fluxes of galactic cosmic rays and the minima of solar activity, beginning from 1958 (according to the data of a cosmic ray monitor in Kiel, Germany, and the National Geophysical Data Center (NGDC), USA [33].

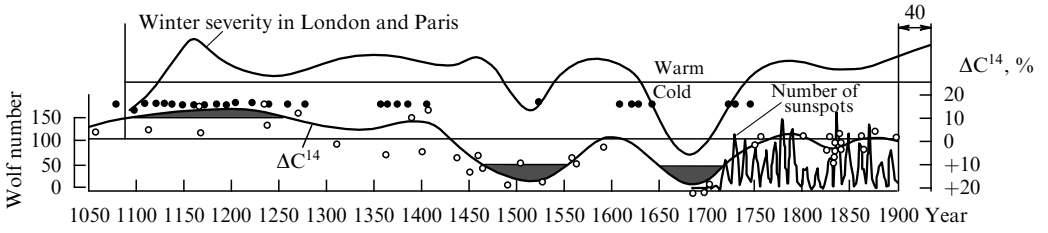

Figure 11. Variations of solar activity level over the past 900 years in comparison with the severity of winters in London and Paris. Also given is the negative value of C^{14} content variation, which correlates with the low intensity of galactic cosmic rays and a high solar activity [35].

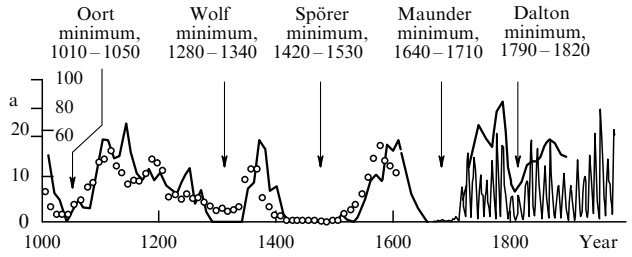

Figure 12. Anomalous periods of low solar activity over the past millennium [36].

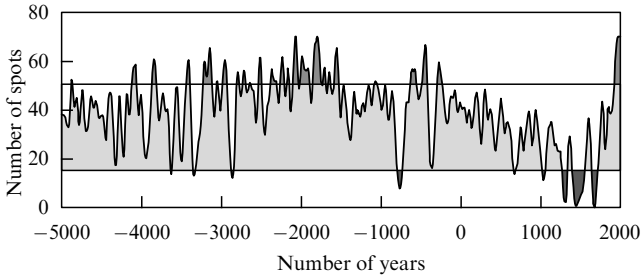

Figure 13. Reconstruction of solar activity to the distant past [37] (the beginning of the Common Era is taken as the zero on the time scale).

of solar energy that reaches Earth. This hypothesis is presently being verified in the Cloud experiment at the CERN accelerator: an air-filled chamber is irradiated by high-energy particle fluxes [34].

From direct and indirect data it was established that anomalies in the behavior of solar activity frequently occurred. The periods of low solar activity are shown in Fig. 12. The global minima of these solar activity minima are spaced in time by about 200 years, and they are associated with the lower-temperature periods. This brings up the natural question: are these periods likely to recur and, if yes, when are they to be expected?

A reconstruction exists of the solar activity level to a more distant past, as far as 5000 years B.C. [37] (Fig. 13). Enhanced activity periods were succeeded by low-activity ones. This behavior of the Sun is associated, one way or another, with the action of the solar dynamo. Nowadays, we see an increase in solar activity and its related warming, which should, by analogy with the past periods, be succeeded by a lowering of solar activity and of the temperature. Nevertheless, seriously being debated are, apart from natural factors, climate changes arising from anthropogenic factors — industrial CO_2 emissions — which is the subject of comprehensive studies [32].

4. Conclusions

Progress in the study of physical processes in the Sun–Earth system depends to a large measure on the acquisition of new data, which also involves spacecraft-based observations and measurements. Recent years have seen the implementation of the national CORONAS-I, Interbol, CORONAS-F, and CORONAS-PHOTON projects [38, 39], as well as of a series of projects drawn up by the space agencies of the USA, Europe, and Japan [40, 41]. The national Rezonans and Intergelioprobe projects [40–42], which are aimed at obtaining new data in the area of solar–terrestrial physics, will investigate the entire chain of processes — from the processes in the Sun to those in the terrestrial magnetosphere.

To summarize, it is pertinent to note that research in the scientific area of solar–terrestrial physics, to which V V Migulin devoted much effort and many years of his life, continues to advance at a rapid pace and is yielding new, interesting results, including those for practical applications.

References

1. Baker D N et al. (Eds) *Solar Dynamics and Its Effects on the Heliosphere and Earth* (Dordrecht: Springer, 2007)
2. Kuznetsov V D *Usp. Fiz. Nauk* **176** 319 (2006) [*Phys. Usp.* **49** 305 (2006)]
3. Gavrin V N et al., in *Neutrino 90*: *Intern. Conf. on Neutrino Physics and Astrophysics, Geneva, Switzerland, 10–15 June 1990*; Abazov A I et al. *Nucl. Phys. B Proc. Suppl.* **19** 84 (1991)
4. Kosovichev A G, Duvall T L (Jr.), Scherrer P H *Solar Phys.* **192** 159 (2000)
5. Miesch M S *Astron. Nachr.* **328** 998 (2007)
6. Penn M J, Livingston W *Proc. IAU* **6** 126 (2010)
7. Kuznetsov V D, in *Plazmennaya Geliogeofizika* (Plasma Heliogeophysics) Vol. 1 (Eds L M Zelenyi, I S Veselovsky) (Moscow: Fizmatlit, 2008) p. 81
8. Migulin V V, Molodenskii M M, Syrovatskii S I *Vestn. Akad. Nauk SSSR* (5) 59 (1979)
9. Zeldovich Ya B, Ruzmaikin A A, in *Vspyshki na Zvezdakh* (*Sverkhnovye, Rentgenovskie Istochniki. Solntse)* (Stellar Flares (Supernovae, X-Ray Sources. The Sun)) (Itogi Nauki i Tekhniki. Ser. Astron., Vol. 21) (Moscow: VINITI, 1982) p. 151 [*Sov. Sci. Rev. Astron.* **2** 333 (1983)]
10. Kuznetsov V D *Usp. Fiz. Nauk* **180** 554 (2010) [*Phys. Usp.* **53** 528 (2010)]
11. Frank Hill et al., in *Ann. Meet. Solar Physics Division American Astronomical Society, Las Cruces, NM, June 13–16, 2011*, Presentation 16.10
12. Hecht L "To be or not to be: A galactic question", Booklet of the Citizens Electoral Council of Australia (2011) p. 48
13. Altrock R *ASP Conf. Ser.* **428** 147 (2010)
14. Dikpati M, in *Selected Papers from the 2007 Kyoto Symp.* (Eds T Tsuda et al.) (Kyoto, 2007) p. 171
15. Bothmer V, Daglis I A *Space Weather — Physics and Effects* (Chichester: Praxis Publ., 2007)
16. Elias A G, Silbergleit V M *Prog. Electromagn. Res. Lett.* **1** 139 (2008)
17. Kuznetsov V D, Makhutov N A *Vestn. Ross. Akad. Nauk* **82** 110 (2012) [*Herald Russ. Acad. Sci.* **82** 36 (2012)]
18. Larose D, IEEE Special Publication 90TH0291-5 PWR (1989) p. 10
19. Carrington R C *Mon. Not. R. Astron. Soc.* **20** 13 (1860)
20. Cliver E W *Adv. Space Res.* **38** 119 (2006)
21. Cliver E W, Svalgaard L *Solar Phys.* **224** 407 (2004)
22. Boteler D H *Adv. Space Res.* **26** (1) 15 (2000)
23. Bloxham J, Gubbins D *Sci. Am.* **261** (12) 68 (1989)
24. Cox A *Plate Tectonics and Geomagnetic Reversals* (San Francisco: W.H. Freeman, 1973)
25. Barton C E, in *The Encyclopedia of Solid Earth Geophysics* (Ed. D E James) (New York: Van Nostrand Reinhold, 1989) p. 560
26. Olsen N *Eos Trans. AGU* **88** 293 (2007)
27. Zvereva T I *Geomagn. Aeronom.* (2012) (in press)
28. *Severe Space Weather Events — Understanding Societal and Economic Impacts. A Workshop Report* (Washington, DC: The National Academies Press, 2009)
29. Jackman C H, McPeters R D *Solar Variability Effects Climate Geophys. Monograph* **141** 305 (2004)
30. Wilcox J M et al. *J. Atm. Sci.* **31** 581 (1974)
31. Prikryl P, Rušin V, Rybanský M *Ann. Geophys.* **27** 1 (2009)
32. Idso C, Singer S F *Climate Change Reconsidered. 2009 Report of the Nongovernmental International Panel on Climate Change* (*NIPCC*) (Eds J L Bast, D C Bast) (Chicago: The Heartland Institute, 2009)
33. "Solar activity: Cosmic ray intensity and sunspot activity", http://www.climate4you.com/Sun.htm
34. Kirkby J et al. *Nature* **476** 429 (2011)
35. Eddy J A *Science* **192** 1189 (1976)

36. Eddy J A, in *The Ancient Sun*: *Fossil Record in the Earth, Moon, and Meteorites*: *Proc. of the Conf., Boulder, Colorado, October 16 – 19, 1979* (Eds R O Pepin, J A Eddy, R B Merrill) (Oxford: Pergamon Press, 1980) p. 119
37. Usoskin I G, Solanki S K, Kovaltsov G A *Astron. Astrophys.* **471** 301 (2007)
38. Kuznetsov V D (Ed.) *Solnechno-Zemnaya Fizika*: *Rezul'taty Eksperimentov na Sputnike KORONAS-F* (Solar-Terrestrial Physics: Results of CORONAS-F Satellite-Based Experiments) (Moscow: Fizmatlit, 2009)
39. Kuznetsov V D, Zhitnik I A, Sobel'man I I *Vestn. Ross. Akad. Nauk* **75** 704 (2005) [*Herald Russ. Acad. Sci.* **75** 370 (2005)]
40. Kuznetsov V D *Usp. Fiz. Nauk* **180** 988 (2010) [*Phys. Usp.* **53** 947 (2010)]
41. Kuznetsov V D, in *Pyat'desyat Let Kosmicheskikh Issledovanii*: *po Materialam Mezhdunar. Foruma ''Kosmos*: *Nauka i Problemy XXI Veka'', Oktyabr' 2007 Goda, Moskva* (Fifty Years of Space Research: the International Forum "Space: Science and Problems of the 21st Century", October 2007, Moscow) (Ed. A V Zakharov) (Moscow: Fizmatlit, 2009) p. 60
42. Kuznetsov V D, Zelenyi L M, in *Solnechno-Zemnaya Fizika* (Solar-Terrestrial Physics) Issue 12 *Trudy Mezhdunar. Simpoziuma ''Mezhdunarodnyi Geliofizicheskii God — 2007*: *Novyi Vzglyad na Solnechno-Zemnuyu Fiziku'', Zvenigorod, 5–11 Noyabrya 2007 g.* (Proc. Intern. Symp. "Intern. Heliophysical Year – 2007: New Glance at Solar-Terrestrial Physics", Zvenigorod, 5–11 November 2007) Vol. 1 (Novosibirsk: Inst. Solnechno-Zemnoi Fiziki RAN, 2008) p. 83